

Optimal Microgrid Scheduling with Peak Load Reduction Involving an Electrolyzer and Flexible Loads

Lucas Bolivar Jaramillo¹, Anke Weidlich^{1,*}

Abstract

This work consists of a multi-objective mixed-integer linear programming model for defining optimized schedules of components in a grid-connected microgrid. The microgrid includes a hydrogen energy system consisting of an alkaline electrolyzer, hydrogen cylinder bundles and a fuel cell for energy storage. Local generation is provided from photovoltaic panels, and the load is given by a fixed load profile combined with a flexible electrical load, which is a battery electric vehicle. The electrolyzer has ramp-up constraints which are modelled explicitly. The objective function includes, besides operational costs and an environmental indicator, a representation of peak power costs, thus leading to an overall peak load reduction under optimized operation. The model is used both for controlling a microgrid in a field trial set-up deployed in South-West Germany and for simulating the microgrid operation for defined period, thus allowing for economic system evaluation. Results from defined sample runs show that the energy storage is primarily used for trimming the peak of electricity drawn from the public grid and is not solely operated with excess power. The flexible demand operation also helps keeping the peak at its possible minimum.

Keywords: Microgrid scheduling, Peak power reduction, Energy storage, Ramp-up constraints, MILP, Alkaline electrolysis, Demand response

*Corresponding author

¹University of Applied Sciences, Institute of Energy Systems Technology, Badstr. 24, 77652 Offenburg, Germany

©2016. This manuscript version is made available under the CC-BY-NC-ND 4.0 license <http://creativecommons.org/licenses/by-nc-nd/4.0/>

DOI: <https://doi.org/10.1016/j.apenergy.2016.02.096>

Preprint submitted to Applied Energy – Accepted Manuscript

1. Introduction

The efforts to make the electrical grid more reliable even with high shares of renewable energy have led to the concepts of smart grids and microgrids. A smart grid is an electricity system that uses modern information and communication technology (ICT) for better managing grid operation and balancing demand and supply. Microgrids, in contrast, can be defined as local clusters of distributed energy resources and loads connected by a distribution system, usually at medium or low voltage, that can work disconnected or connected to the main grid (connected or islanded mode of operation) [1–5]. One characteristic aspect of many microgrids is the integration of renewable energy, distributed generation and storage for better serving the local demand at a specific site. This is usually facilitated by ICT and algorithms for optimizing the energy flows and the use of locally available energy. Since microgrids can – entirely or partially – meet this on-site energy demand, the main grid is eased of this load [6], leading to a less stressed overall system.

Growing demand for electricity has a direct impact on the peak consumption, which entails high investment costs for peak power facilities that have rather low operating hours. The increased use of electric vehicles (EVs) can further increase peak power demand, since an EV alone can require as much power as a typical home [7]. The additional load from uncontrolled charging of electric vehicles could increase the peak demand by up to 20 %, depending on EV diffusion [8, for the case of New Zealand]. Peak control therefore becomes an important objective. Microgrids can contribute to peak control by implementing demand response strategies for flexible loads, i. e. influencing the operation of either shiftable or controllable loads to better match local generation [9].

Given the challenges of electricity systems and the capabilities of microgrids as described above, the goal of this work is to optimize the operation of a microgrid, allowing for cost minimization, peak power reduction and minimal greenhouse gas emissions simultaneously. To this end, a multiple objective mixed-integer linear programming problem is formulated that finds optimized schedules for the different components of the microgrid. The system includes energy storage in the form of a hydrogen system: in times of available excess electricity, hydrogen is produced by an electrolyzer and subsequently stored; during a shortage of supply from the local photovoltaic panel, the hydrogen can be reconverted into electricity by means of a fuel cell. The electrolyzer is of alkaline type. As the alkaline water electrolysis cannot operate imme-

diately after a cold start of the apparatus, the time needed for ramping up the system must be taken into account in the optimization model. Besides, frequent starts and stops of the electrolyzer and fuel cell should be avoided in order to reduce wear.

Many models have been developed for optimizing multiple objectives in microgrid operation, e. g. for simultaneous minimization of operational costs and emissions [1, 10–12]. Some models include start-up costs for single components in order to avoid frequent starts and stops in the operation of the component [1, 10, 12]. Others consider demand response for peak power shaving, e. g. [9, 13–15]. To the knowledge of the authors, there are hardly any microgrid models that represent the specifics of energy storage in form of a hydrogen system. In particular, ramp-up constraints are not considered in other microgrid models. This latter aspect, in combination with the aforementioned peak load reduction, avoidance of frequent component starts and stops and the integration of flexible loads makes the model presented here extremely flexible. It is suitable for representing the microgrid with hydrogen system studied in this work, but also allows for modeling other system configurations (including, e. g., polymer electrolyte membrane (PEM) electrolysis, battery storage, wind generation,...) by adapting the according parameter values of the components. The model can then be used both for actually controlling a microgrid based on load and generation forecasts, and for simulating the microgrid operation for a defined time horizon.

The remainder of the paper is structured as follows: In Section 2 the multiple objective MILP microgrid model is described and all relevant equations are given. Section 3 contains the results from well-defined scenario runs, which are then discussed in Section 4. Finally, Section 5 concludes the findings.

2. The Model

This section describes the system under study (2.1) and provides the mathematical equations defining the objective function and constraints of the multi-objective MILP (2.2).

2.1. The Microgrid System

The modeled system is a physical microgrid installation at the Institute of Energy Systems Technology, situated in the South-West of Germany. It has a connection to the public electricity grid and consists of a set of photovoltaic

(PV) panels, a hydrogen storage system (HYS) as well as fixed and flexible loads. The HYS consists of an alkaline electrolyzer, hydrogen cylinder bundles and a fuel cell. A battery electric vehicle (BEV) represents the flexible load. The fixed load is given by the electrical appliances of the connected office building, represented by a G1 profile as provided by BDEW [16]. Figure 1 shows the energy flows of the modeled system. Some characteristics of the elements are described in Table 1.

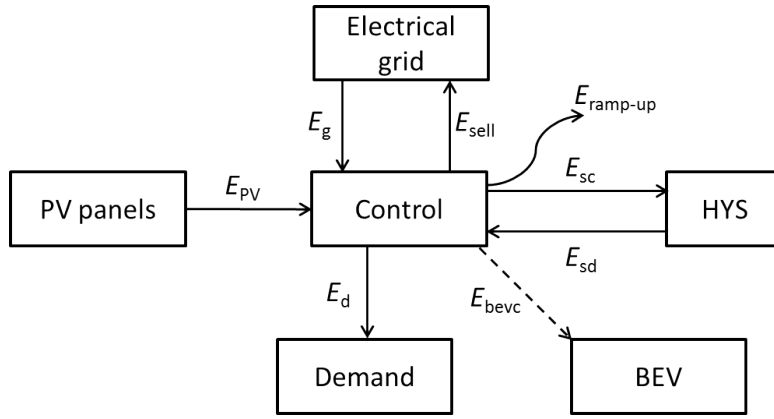


Figure 1: Sketch of the energy flows in the microgrid

Table 1: Microgrid units specification

Element	Power (in kW)	Capacity (in kWh)
PV	12.8	--
Electrolyzer	6.0	--
Fuel cell	1.7	--
Hydrogen storage	--	50
BEV	80	24

2.2. Mathematical Formulation

The main unit used in the model is (electrical) energy E per time interval t . Only in the case of the hydrogen storage content, E_s represents the accumulated energy contained in chemical form in the storage cylinders. The objective of microgrid scheduling is to simultaneously minimize operational

costs and the environmental impact of microgrid operation. The cost is defined by the amount of energy bought from the grid (E_g , with per-unit cost of usage c_g), start-up costs for the electrolyzer and the fuel cell (c_{sc} and c_{sd} ; the subscript parts c and d stand for charging and discharging, respectively, for representing generic storage technologies), the energy injected into the public grid (E_{sell} , with feed-in tariff c_{sell} , negative cost) and the peak power drawn, P_{peak} , with per-unit cost c_{peak} . Given that the electricity mix in most countries involves considerable greenhouse-gas emissions (as opposed to the local PV generation), the environmental impact is assessed by the use of energy drawn from the grid.

The fixed demand E_d , the electricity generation from the PV panels E_{PV} and the times at which the BEV is plugged to the microgrid for charging as well as its respective arrival and departure states of charge (SOC) are known. The other energy flows are calculated by the MILP solver. Energy flowing into the microgrid (see Figure 1) is considered positive, and energy flowing out of the microgrid is denoted by negative values. In Equation 1, all variables are calculated for each time step, except the peak power P_{peak} , which is only the highest value of power needed from the grid in the evaluated period.

$$\text{Min } z = \sum_{t=1}^T \left\{ \lambda_1 \left(\frac{c_g E_{g,t} + c_{sc} S_{upc,t} + c_{sd} S_{upd,t} - c_{sell} E_{sell,t} + c_{peak} P_{peak}}{\Omega} \right) + \lambda_2 \frac{E_{g,t}}{\Phi} \right\} \quad (1)$$

Here, S_{upc} and S_{upd} are binary variables that represent starting up the hydrogen storage system for charging and discharging, respectively. λ_1 and λ_2 are the weighting factors of this multiple objective problem. Ω and Φ are normalizing terms used in order to get dimensionless expressions for the cost and emissions part, with Ω representing the cost of buying the complete fixed demand from the grid, and Φ representing the emissions associated with meeting the fixed demand entirely with energy from the grid.² Unless stated otherwise, all constraints are valid $\forall t \in [1, T]$, with one time step t representing a 15 min interval. All variables are positive and all variables denoted with S are binary variables, i. e. $\in \{0, 1\}$.

² Φ must therefore include the CO₂ emission factor of the grid energy, which would be in the order of $0.67 \frac{\text{kg CO}_2}{\text{kWh}}$ for the example of the German power mix [17]. It has to be noted, however, that this factor appears both in the indicator and the denominator, and is therefore cancelled out.

The electrolyzer needs k time steps for being operational. The alkaline electrolyzer modeled here needs up to 45 minutes, i. e. three time steps for inertization, pressurization and other preparatory activities. During this time, energy is consumed, but no hydrogen is produced. Figure 2 shows how the energy input to the electrolyzer E_{sc} , the binary variables for starting up the electrolyzer S_{upc} , for operating S_{sc} , and for shutting down the electrolyzer S_{downc} are related for $k = 3$. The start-up variable for charging has a value of one only in the moment in which the system goes into the charging mode, and is zero otherwise. The shut-down variable for charging has a value of one only when the system stops charging (the same logic applies to the discharging, i. e. fuel cell variables). The variable for charging S_{sc} has a value of 1 at all times that the electrolyzer is working, from start-up to shut-down (the same works for discharging variable S_{sd}).

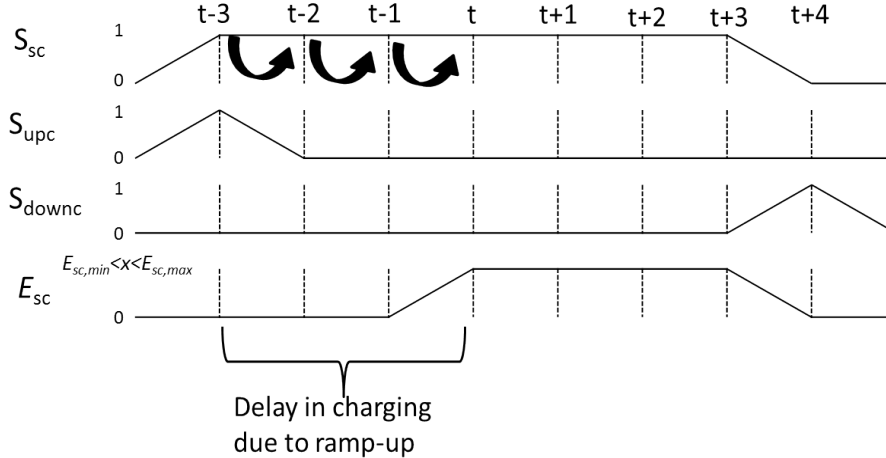


Figure 2: Behaviour of binary variables for when hydrogen production starts (for $k = 3$)

Expressions 2 and 3 represent the constraint of maximum and minimum energy that can be fed into the HYS ($E_{sc,min}$, $E_{sc,max}$) and withdrawn from it ($E_{sd,min}$, $E_{sd,max}$), which corresponds to the maximum and minimum power that the electrolyzer can draw and the fuel cell can provide. Expression 4 represents the constraint that the maximum energy storage capacity E_s cannot be exceeded.

$$E_{sc,\min} (S_{sc,t-k} - S_{downc,t-(k-1)} - \dots - S_{downc,t}) \leq E_{sc,t} \leq E_{sc,\max} (S_{sc,t-k} - S_{downc,t-(k-1)} - \dots - S_{downc,t}), \forall t \in [k+1, T] \quad (2)$$

$$E_{sd,\min} S_{sd,t} \leq E_{sd,t} \leq E_{sd,\max} S_{sd,t} \quad (3)$$

$$E_{s,t} \leq E_{s,full} \quad (4)$$

The processes of starting-up and shutting-down exclude one another; this is shown in Expressions 5 and 6 for charging and discharging, respectively. Equations 7 and 8 define the starting-up and shutting-down of the charging and discharging process [12].

$$S_{upc,t} + S_{downc,t} \leq 1 \quad (5)$$

$$S_{upd,t} + S_{downd,t} \leq 1 \quad (6)$$

$$S_{sc,t-1} - S_{sc,t} = S_{downc,t} - S_{upc,t}, \forall t \in [2, T] \quad (7)$$

$$S_{sd,t-1} - S_{sd,t} = S_{downd,t} - S_{upd,t}, \forall t \in [2, T] \quad (8)$$

Equation 9 represents the overall energy balance (see also Figure 1). E_{PV} and E_d are fixed inputs taken from measurements and standard load profiles, respectively. E_{ramp_up} represents the fixed energy that the electrolyzer consumes per time step of starting up. As the ramp-up term is valid only from time step k onwards, the energy balance equation is differentiated for the very first time steps and afterwards. The balance in the hydrogen energy storage is shown in Equation 10. Figure 3 illustrates the HYS energy balance. The hydrogen storage level at $t = 1$ is given as a fixed input.

$$E_{PV,t} - E_{d,t} - E_{sc,t} + E_{sd,t} + E_{g,t} - E_{sell,t} - E_{bevc,t} = 0, \forall t \in [1, k-1]$$

$$E_{PV,t} - E_{d,t} - E_{sc,t} + E_{sd,t} + E_{g,t} - E_{sell,t} - E_{bevc,t} - E_{ramp_up} (S_{upc,t} + S_{upc,t-1} + \dots + S_{upc,t-(k-1)}) = 0, \forall t \in [k, T] \quad (9)$$

$$E_{s,t} = E_{s,t-1} + E_{sc,t-1} \cdot \eta_{ely} - \frac{E_{sd,t-1}}{\eta_{fc}}, \forall t \in [2, T] \quad (10)$$

The state of charge (SOC) of the BEV is known at its arrival and departure times. At times when the BEV is plugged to the microgrid, the binary

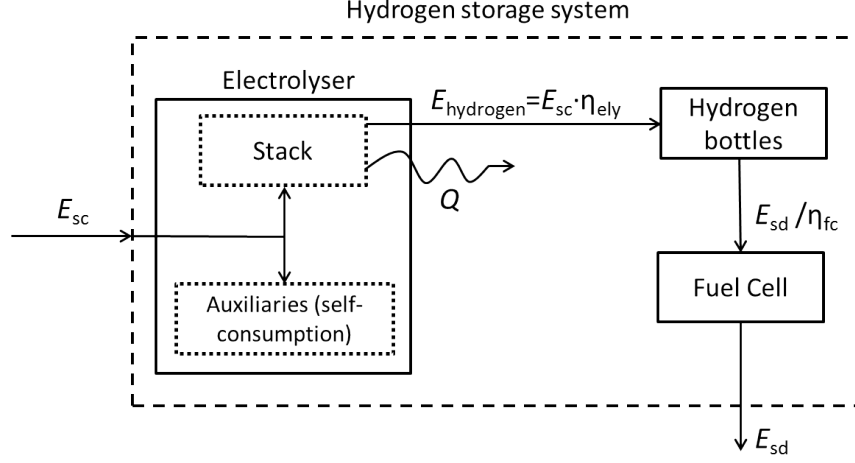


Figure 3: Hydrogen storage system.

variable S_{bev} can take both values 0 and 1; when the car is on a trip, S_{bev} is always 0 (Expression 11). It can charge any energy amount $E_{bev,t}$ per time step between a maximum and minimum value (Expression 12). Discharging is not considered, i. e. the BEV does not provide energy to the microgrid. The energy content of the BEV battery $E_{bev,t}$ is zero when the BEV is on a trip, because it plays no part in the microgrid during such period. t_{in} and t_{out} are the time steps at which the BEV is available for charging and required to go to the next trip, respectively. The numeric subscript in this terms refers to how many times the BEV goes into the microgrid for charging during the simulation period, that is 1 for the first time, 2 for the second time, and so on. The times during which the BEV is available are contained within the interval with subscript in and out . Expression 13 defines the energy content of the BEV battery at all periods and how it is related to the charge energy $E_{bev,t}$.

$$S_{bev,t} \in \begin{cases} \{0, 1\} & \text{if } t \in [t_{in,1}, t_{out,1}) \cup [t_{in,2}, t_{out,2}) \cup \dots \cup [t_{in,n}, t_{out,n}) \\ \{0\} & \text{if otherwise} \end{cases} \quad (11)$$

$$E_{bev,\min} S_{bev,t} \leq E_{bev,t} \leq E_{bev,\max} S_{bev,t} \quad (12)$$

$$E_{\text{bevs},t} = \begin{cases} E_{\text{bevs},in,1} & \text{if } t = t_{in,1} \\ E_{\text{bevs},in,2} & \text{if } t = t_{in,2} \\ \dots & \dots \\ E_{\text{bevs},in,n} & \text{if } t = t_{in,n} \\ E_{\text{bevs},out,1} & \text{if } t = t_{out,1} \\ E_{\text{bevs},out,2} & \text{if } t = t_{out,2} \\ \dots & \dots \\ E_{\text{bevs},out,n} & \text{if } t = t_{out,n} \\ E_{\text{bevs},t-1} + E_{\text{bevc},t-1} & \text{if } t \in (t_{in,1}, t_{out,1}) \cup (t_{in,2}, t_{out,2}) \cup \dots \cup (t_{in,n}, t_{out,n}) \\ 0 & \text{if otherwise} \end{cases} \quad (13)$$

$$E_{g,t} \frac{3600}{\Delta t} \leq P_{\text{peak}} \quad (14)$$

The last expression (14) refers to the objective to limit the maximum power drawn from the grid during the whole time horizon. The factor $3600/\Delta t$ calculates the average power drawn per time interval, with $\Delta t = 900$ sec (15 minutes) [13, 14].

3. Simulation Results

Model validation and analysis has been done based on reference simulation runs using the Matlab Global Optimization Toolkit. Table 2 gives the per-unit costs and the performance parameters applied. The 15 min values for PV production are given based on [18]; the data representing the fixed 15 min demand is based on the standard load profile G1 provided by BDEW (German Association of the Energy and Water Industry, former VDEW; the G1 profile specifies the average electric load of offices and businesses with a yearly consumption of less than 100 MWh, operating from 08:00 am to 06:00 pm) [16]. PV production and fixed demand are displayed in Figure 4 for a two week period. The data representing the BEV trip times and the required SOC for each trip start are shown in Table 3.

Table 2: Parameters used for simulation runs

Parameter	Value	Units
Cost of energy from the grid c_g	0.25	e/kWh
Feed-in tariff c_{sell}	0.12	e/kWh
Cost of starting up the electrolyzer c_{sc}	0.8	e
Cost of starting up the fuel cell c_{sd}	0.3	e
Cost of peak power c_{peak}	20	e/kWh
Maximum capacity of hydrogen storage $E_{s,full}$	50	kWh
Energy for ramping up the electrolyzer $E_{ramp-up}$	900	Wh
Minimum energy to run the electrolyzer $E_{sc,min}$	300	Wh
Maximum energy to run the electrolyzer $E_{sc,max}$	1500	Wh
Minimum energy output of the fuel cell $E_{sd,min}$	85	Wh
Maximum energy output of the fuel cell $E_{sd,max}$	425	Wh
Minimum energy for charging BEV $E_{bevc,min}$	165	Wh
Maximum energy for charging BEV $E_{bevc,max}$	1650	Wh
Initial state of hydrogen storage	500	Wh
Efficiency electrolyzer η_{ely}	58	%
Efficiency fuel cell η_{fc}	60	%
Weighting factor λ_1	0.7	
Weighting factor λ_2	0.3	

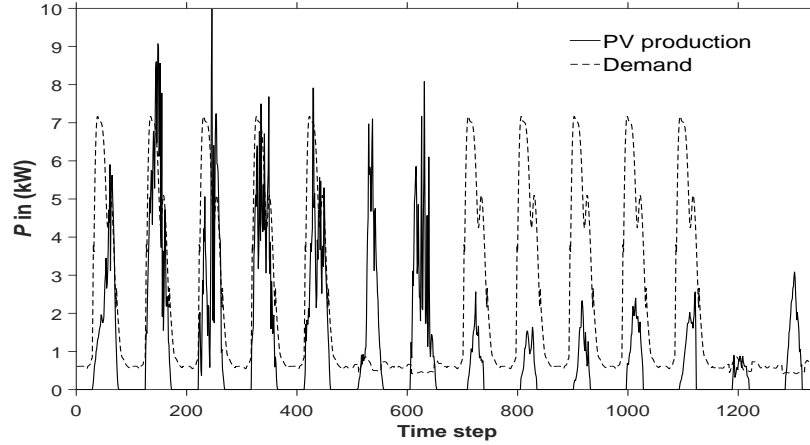


Figure 4: PV production and fixed demand for Case 1

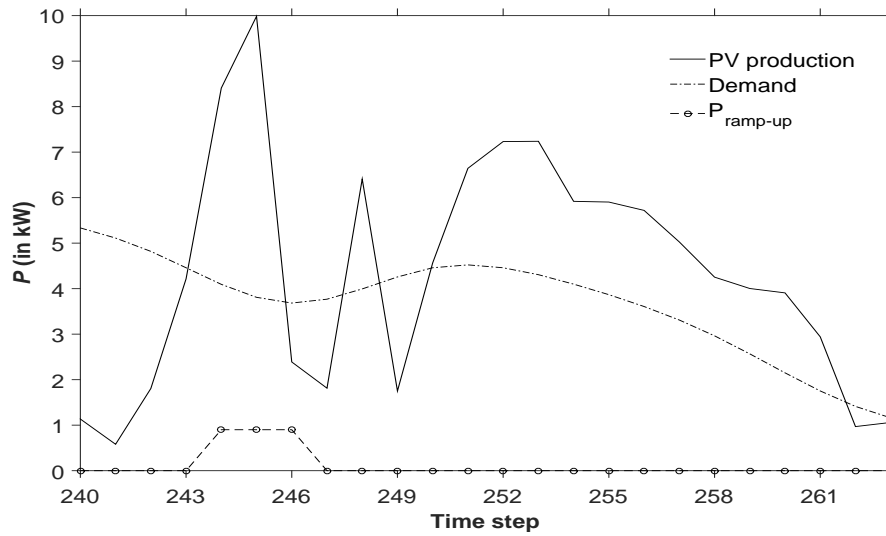
Table 3: BEV trip time steps and according SOC values

t_{in}	t_{out}	$SOC_{in}(\%)$	$SOC_{out}(\%)$
51	237	1	100
241	263	90	100
323	341	1	100
349	523	10	100
535	543	80	99
553	629	5	100
639	649	50	98
709	737	5	100
753	817	10	100
1011	1197	1	100
1201	1223	90	100
1283	1301	1	100
1309	1335	10	100

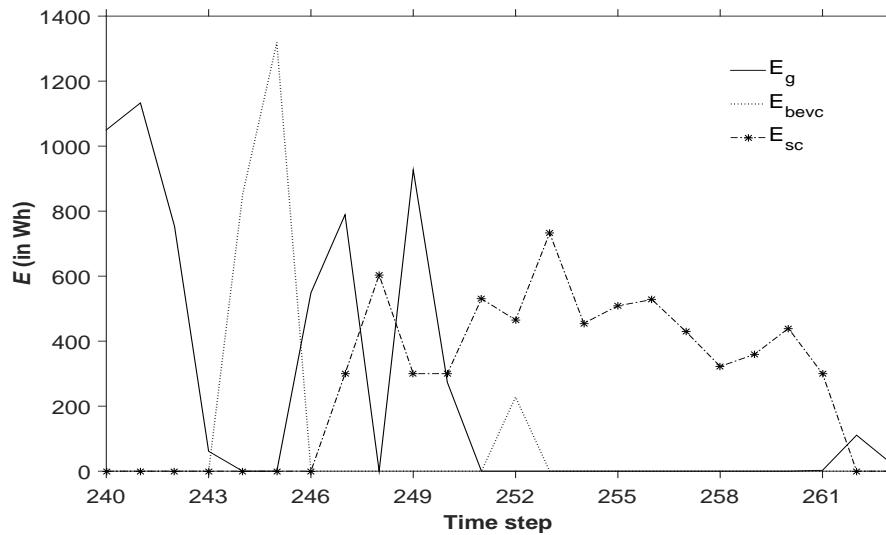
3.1. Reference Case: Case 1 – Full set of Constraints

The operation of the electrolyzer is analyzed here for the time steps 240–263 (Figure 5). It first ramps up in time steps 248 to 250 (see Figure 5(a)) and then starts producing hydrogen in time steps 251 to 261 (Figure 5(b)), confirming that the delay in the hydrogen production after start-up is correctly modelled. When PV production is less than the fixed demand, the differences are covered by the grid; the grid also partly supplies the electrolyzer during this time, avoiding another start-up for using the excess energy occurring again in time steps 251–261. So, the electrolyzer is not solely operated in times of excess PV energy, but the solver may decide to provide the minimum electrolyzer energy (0.9 kWh for ramp-up and 0.3 Wh for charging the HYS, per 15 min) partly from the grid if that allows better use of excess energy in other time steps and avoids start-up and shut-down operations. The BEV is charged in time steps 244 and 245 and in time step 248, when higher excess energy from PV takes place.

Between time steps 705 and 740 an extreme case of demand is observed (Figure 6). The PV production is much lower than the demand and the BEV needs to charge 22.8 kWh within this period. Besides, the period corresponds to the highest fixed demand, thus contributing much to the overall peak load. In this case, energy from the grid is needed to cover both fixed and flexible



(a)



(b)

Figure 5: Microgrid operation at time steps 240 to 263: (a) PV production, demand and ramp-up; (b) energy from the grid, energy into BEV (flexible demand), energy into electrolyzer

demand. In order to avoid a high peak of energy drawn from the grid, the fuel cell enters into operation at time step 709 and works until time step 736

at full capacity (1.7 kW or 425 Wh for each 15-minute interval). Also, the system makes use of the given demand flexibility, and charges the BEV at the lowest possible power when the residual load is high, in order to avoid increasing the peak power drawn from the grid.

3.2. Case 2 – Without BEV

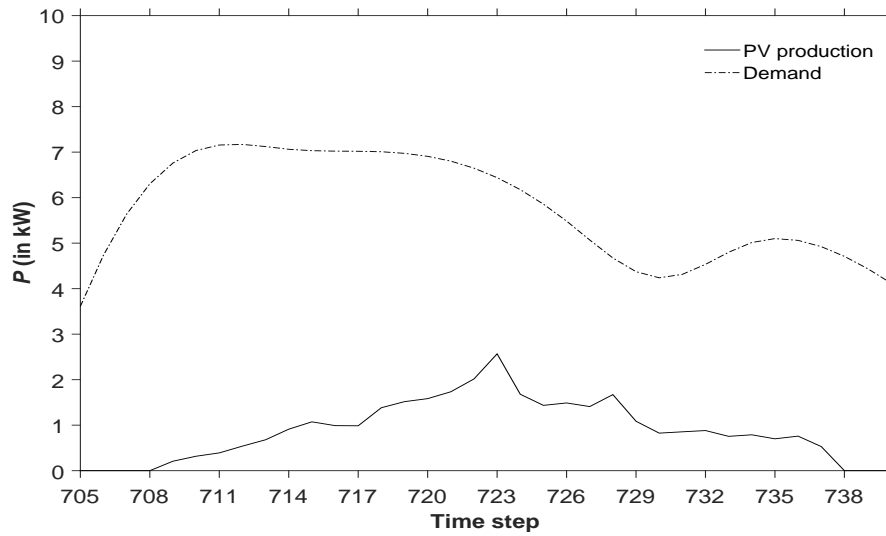
Case 2 is the same as Case 1, except that the BEV is not taken into consideration. The evolution of the hydrogen storage content for both cases is shown in Figure 7. It can be observed that hydrogen was stored in three occasions in Case 1, and twice in Case 2. Hydrogen consumption for the fuel cell occurred five times in both cases. These discharging events correspond to an interval of high fixed demand. The amount of hydrogen stored in Case 2 is higher than in Case 1 due to the absence of the BEV, which leaves more excess energy for the electrolyzer. Around time step 240, the excess energy in Case 2 is sold rather than stored in BEV, as happened in Case 1 (cp. Figures 7 and 5(b)). Figure 8 shows the behaviour of the energy drawn from the grid for both cases during time steps 700 to 1000. The higher peaks occurring in Case 1 correspond to times when the BEV was charged (around time steps 700 and 800) and also to less energy produced by the fuel cell (discharge of the hydrogen storage).

3.3. Case 3 – Without Peak Power Constraint

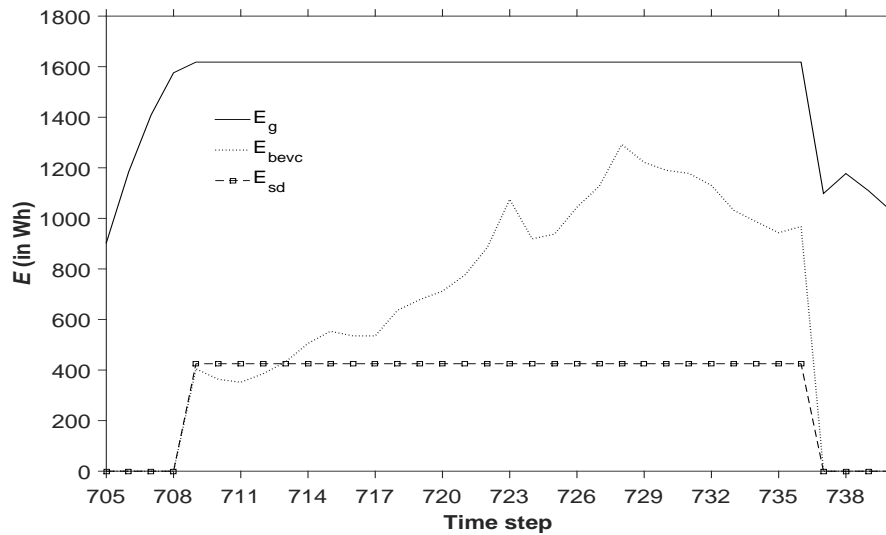
Case 3 differs from the reference case in that the peak power cost is not considered in the objective function. Results show that the hydrogen system is not used for energy storage at all in this case. All excess energy is sold to the grid or used for charging the BEV. Figure 9 shows the energy drawn from the grid for Case 1 and 3 during time steps 700 to 1010. It can be seen that when the peak restriction is removed, the energy drawn from the grid reaches higher values. The time steps 700–750 show that the peak power in Case 3 is around 60 % higher than in Case 1. Both curves follow the same pattern, except when the electric vehicle is charged or when the fuel cell operates (the latter situation occurs only in Case 1).

3.4. Case 4 – No Photovoltaic Production

Case 4 was executed with same parameters as in Case 1, but the PV production was not taken into consideration. For this case, all electricity to meet fixed and flexible demand must come from the grid. The storage system would not be expected to work at all because there is no excess



(a)



(b)

Figure 6: Zoom into time steps 705 to 740: (a) PV production and demand; (b) energy from the grid, energy into BEV (flexible demand), energy output fuel cell

energy from PV. However the solution shows that the HYS is indeed charged using energy from the grid, which is later discharged to trim the power to be drawn from the grid. Energy is taken into the storage just as much to make

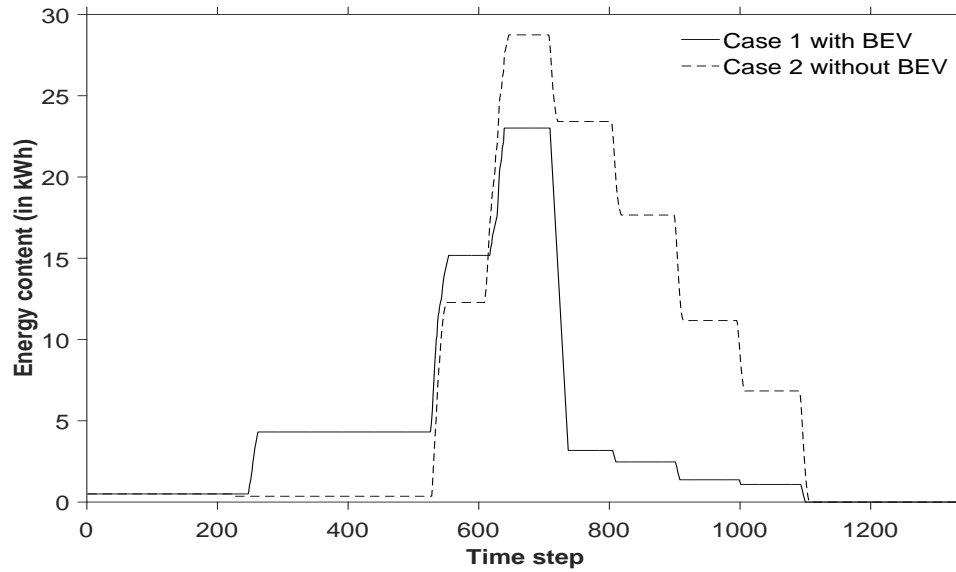


Figure 7: Energy in the hydrogen storage for Cases 1 and 2

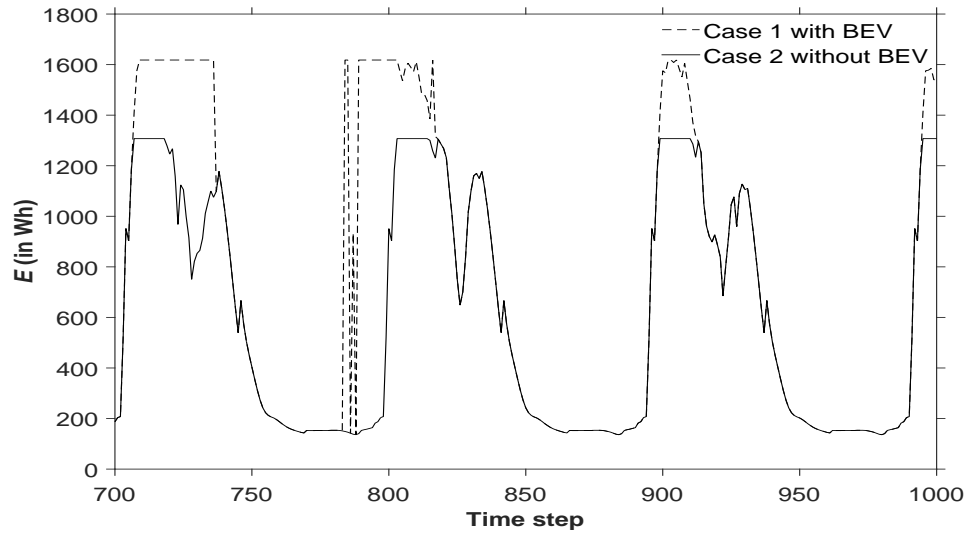


Figure 8: Energy drawn from the grid during time steps 700 to 1000 for Cases 1 and 2

the electricity consumed in that moment to be equal or less than the peak power, and this energy is used when the fixed demand shows a peak and the BEV is in place for charging. The hydrogen is stored in one time interval and consumed in two intervals; this can be seen in Figure 10. Figures 11

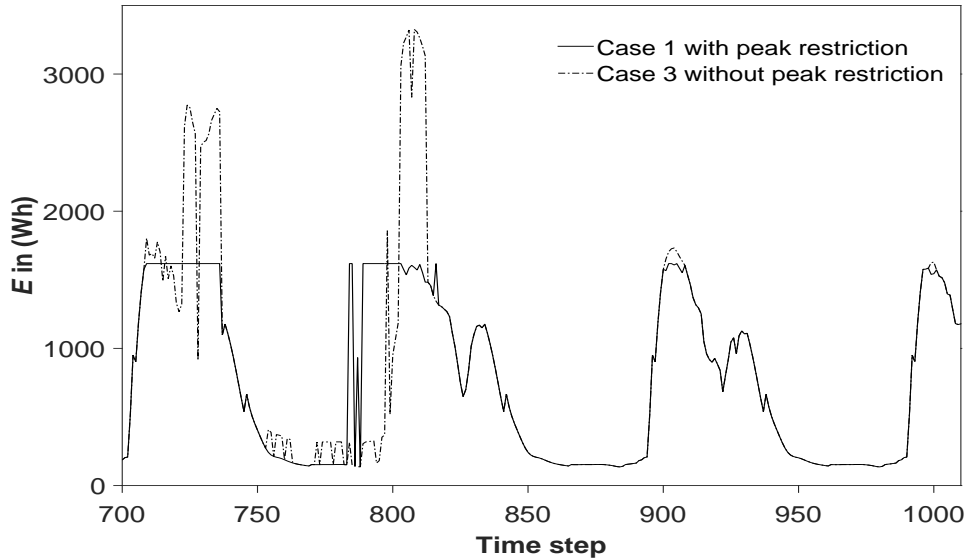


Figure 9: Energy drawn from the grid during time steps 700 to 1010 for Cases 1 and 3

and 12 show the intervals in which the storage is used. It can be seen how the flexible demand also helps to keep the peak power drawn from the grid at its minimum possible, being small when the fixed demand is high and increasing when the other one decreases (time steps 323–332 in Figure 11 and 708–717 in Figure 12). This behaviour is similar to the one shown in Figure 6(b).

Table 4 shows a summary of different variables for Cases 1 to 4. All variables represent the total amounts over the whole analyzed period. C is the total cost of operation during the period, which is formed by the energy taken from the grid, the electricity sold to the grid, start-ups of electrolyzer and fuel cell and the peak power component (numerator of the first part in the objective function).

4. Discussion

The simulation results show how discarding the peak restriction considerably affects the operational cost and also the peak power drawn from the grid (cp. Case 3). This aspect becomes more relevant when a high demand is considered, e. g. including the electric vehicle. The peak power showed an increase of more than 60 % when comparing Cases 1 and 3, while for Case

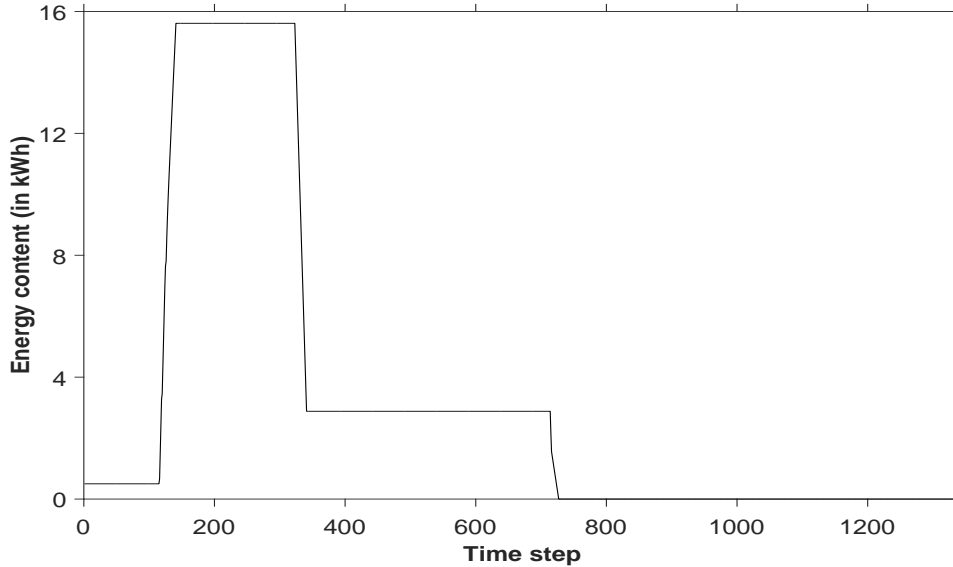


Figure 10: Energy content of hydrogen storage in Case 4

Table 4: Summary results Cases 1–4

Case	Variables							
	C (in e)	E_g (in kWh)	P_{peak} (in kW)	E_{sc} (in kWh)	S_{sc}	S_{upc}	S_{sd}	S_{upd}
1	286	614	6.5	39	79	3	49	5
2	210	428	5.2	49	65	2	71	6
3	372	618	11.1	0	0	0	3	1
4	411	914	9.0	26	81	1	23	2

4 (with no PV production) it increased by only 38 %. It is important to mention, however, that the price to be paid for the peak power is usually not calculated on the basis of a two weeks interval (the time horizon regarded here), but on a yearly basis.

The consideration of the peak restriction also shows the significance of using a storage system. In the presented simulations it was the resource mainly applied in order to reduce electricity drawn from the grid, thus avoiding higher power peaks. These results are in accordance with the ones reported by several authors, e. g. [1, 10, 13–15]. The introduction of an electric vehicle increases the usage of the electrical grid, because PV power cannot satisfy

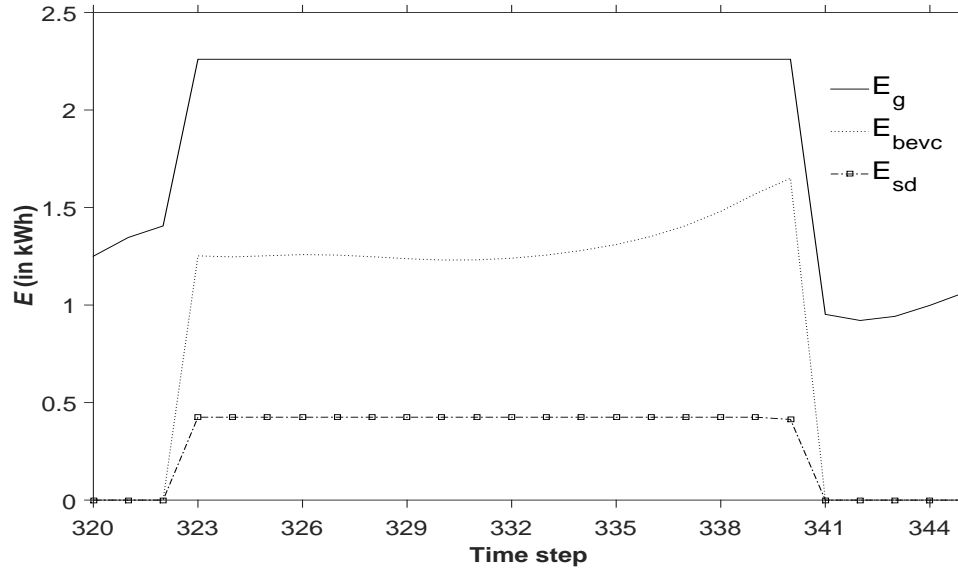


Figure 11: Time steps 320–345: energy from the grid, energy into BEV and output fuel cell in Case 4

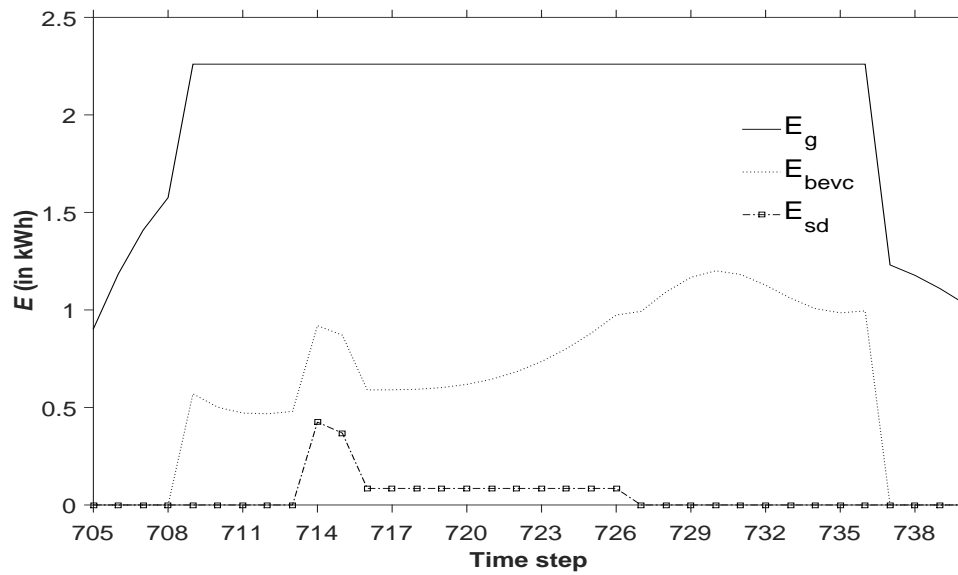


Figure 12: Time steps 705–740: energy from the grid, energy into BEV and output fuel cell in Case 4

this additional demand at all times (Case 1 vs. Case 2). Without the BEV, the system makes more use of the electrolyzer and the fuel cell, as these are then the only flexible components. For Case 1, the electrolyzer runs 26 consecutive intervals per start-up on average. The fuel cell runs almost nine time intervals per start-up (calculated by dividing S_{sc} and S_{sd} by S_{upc} and S_{upd} , respectively). In Case 2, the average running time for electrolyzer was 32 time intervals, and 11 for the fuel cell. In Case 1, the fuel cell discharged at full power 86 % of the energy stored in the hydrogen cylinders between time step 710 and 737 in order to help charge the BEV and avoid high peak power, and the remaining 14 % was discharged at a lower and more even rate during times of peak power in fixed demand. In Case 2, the hydrogen storage was discharged more evenly (cp. Figure 7).

Taking into account the peak variable in the objective function has a big impact on the program's run time. When running the simulation without this constraint it took less than five minutes to reach a solution, whereas three hours or more were needed when also considering the peak variable.

5. Conclusions

An optimization model for the scheduling of the different components of a microgrid was developed. The model considers a weighted objective function minimizing cost of operation and environmental impact. The first part of the objective function consists of the cost of purchased energy from the grid, the start-up cost of a fuel cell and of an alkaline electrolyzer, the cost of peak power and the energy fed into the grid (as negative cost). The second part of the objective function considers only the energy drawn from the public grid. The model also involves the use of a flexible demand represented by a battery electric vehicle. As constraints, the model includes technical restrictions of equipment and energy balances in some of the elements. One important characteristic is that it models a ramp-up period for the electrolyzer, in which it draws power but doesn't produce hydrogen.

Including the start-up costs for the electrolyser and fuel cell were shown to have a positive impact on the smoothness of operation of these components, in that they work as long as possible with the least number of start-ups; this feature is easily replicable for other components that could be added to the microgrid, e. g. diesel generators or boilers. In order to avoid high grid peak power, the system makes use of the flexible demand and the hydrogen storage system. Due to the low power assumed for the fuel cell, this element is

mainly used to avoid peaks instead of avoiding the mere usage of electricity from the grid (for example at night-time with low fixed demand and low BEV charging requirements). In further simulation runs, the sizing of the components could be changed to gain more insight into optimized operation of different system variants.

The simulation reveals that electricity from the grid is used to help the electrolyzer keep running in order to avoid its shut-down during a low or no-PV period, so as to take advantage of the excess energy to come in the subsequent periods. The simulation also showed how the electrolyzer works without any PV production (Case 4), drawing energy from the grid during a period of low demand, which is used later to avoid high peak power. Due to the low global efficiency of the hydrogen storage system (around 35 %), the program tries to avoid using it, because it makes more profit from selling energy. With the inclusion of the peak power into the objective function and the more weight on system autarky, however, the usage of the hydrogen system increases.

Acknowledgements

The research described in this article was carried out in the framework of the project *Kommunaler Energieverbund Freiburg – Demonstrationsbetrieb einer Elektrolyseanlage im Industriegebiet Freiburg Nord zur Verbindung des Stromund Erdgasnetzes und zur Speicherung erneuerbarer Energien*, which was supported by the Federal State of Baden-Württemberg under grant BWE13032. The authors would also like to thank Daniel Woods, M.Sc. for his valuable contributions to the model development.

References

References

- [1] S. Conti, R. Nicolosi, S. Rizzo, H. Zeineldin, Optimal dispatching of distributed generators and storage systems for MV islanded microgrids, *IEEE Transactions on Power Delivery* 27 (3) (2012) 1243–1251.
- [2] R. Gupta, N. Gupta, A robust optimization based approach for microgrid operation in deregulated environment, *Energy Conversion and Management* 93 (2015) 121 – 123.

- [3] E. Sfikas, Y. Katsigiannis, P. Georgilakis, Simultaneous capacity optimization of distributed generation and storage in medium voltage microgrids, *Electrical Power and Energy Systems* 67 (2015) 101 – 113.
- [4] A. Fathima, K. Palanisamy, Optimization in microgrids with hybrid energy systems – a review, *Renewable and Sustainable Energy Reviews* 45 (2015) 431 – 446.
- [5] G. Platt, A. Berry, D. Cornforth, What role for microgrids?, in: F. P. Sioshansi (Ed.), *Smart Grid*, Academic Press, 2012, Ch. 9, pp. 185 – 207.
- [6] K. Zhou, S. Yang, Z. Chen, S. Ding, Optimal load distribution model of microgrid in the smart grid environment, *Renewable and Sustainable Energy Reviews* 35 (2014) 304 – 310.
- [7] S. Hauser, K. Crandall, Smart grid is a lot more than just 'technology', in: F. P. Sioshansi (Ed.), *Smart Grid*, Academic Press, 2012, Ch. 1, pp. 3 – 28.
- [8] M. Hindsberger, J. Boys, G. Ancell, Perfect partners: Wind power and electric vehicles – a New Zealand case study, in: F. P. Sioshansi (Ed.), *Smart Grid*, Academic Press, 2012, Ch. 22, pp. 453 – 477.
- [9] O. Erdinc, Economic impacts of small-scale own generating and storage units, and electric vehicles under different demand response strategies for smart households, *Applied Energy* 126 (2014) 142 – 150.
- [10] S. Conti, R. Nicolosi, S. Rizzo, Optimal dispatching of distributed generators in an MV autonomous micro-grid to minimize operating costs and emissions, in: *2010 IEEE International Symposium on Industrial Electronics (ISIE)*, 2010, pp. 2542–2547.
- [11] A. Costa, A. Fichera, A mixed-integer linear programming (MILP) model for the evaluation of CHP system in the context of hospital structures, *Applied Thermal Engineering* 71 (2014) 921 – 929.
- [12] G. Kopanos, M. Georgiadis, E. Pistikopoulos, Energy production planning of a network of micro combined heat and power generators, *Applied Energy* 102 (2013) 1522–1534.

- [13] Z. Zhu, J. Tang, S. Lambbotharan, W. Chin, Z. Fan, An integer linear programming and game theory based optimization for demand-side management in smart grid, in: GLOBECOM Workshops (GC Wkshps), 2011 IEEE, 2011, pp. 1205–1210.
- [14] H. Sherif, Z. Zhu, S. Lambbotharan, An optimization framework for home demand side management incorporating electric vehicles, in: Innovative Smart Grid Technologies - Asia (ISGT Asia), 2014 IEEE, 2014, pp. 57–61.
- [15] L. Sigrist, E. Lobato, L. Rouco, Energy storage systems providing primary reserve and peak shaving in small isolated power systems: An economic assessment, *Electrical power and energy systems* 53 (2013) 675–683.
- [16] Bundesverband der Energie- und Wasserwirtschaft BDEW, Standardlastprofil Strom G1, published by various DSOs, e. g.
URL <https://www.ewe-netz.de/strom/1988.php>
- [17] M. Brander, A. Sood, C. Wylie, A. Haughton, J. Lovell, Electricity-specific emission factors for grid electricity, Tech. rep., ecometrica (2011).
- [18] K. Böhler, M. Wülker, Weather data at the University of Applied Sciences Offenburg (since 1992), Offenburg.